AIAA JOURNAL
Vol. 35, No. 2, February 1997

Importance of Instability in Impact Response and Damage Resistance of Composite Shells

Brian L. Wardle* and Paul A. Lagace†
Massachusetts Institute of Technology, Cambridge, Massachusetts 02139

The response of laminated cylindrical composite shell structures to transverse loading was studied through impact and quasi-static testing. A highly nonlinear structural instability phenomenon, closely resembling a snap-through instability, was found to have a strong influence on the loading/impact response including the resulting damage. Because of this structural instability, the behavior of convex shells under static or dynamic (i.e., impact) transverse loading is found to be much different than that for plates. These differences include trends displayed in the response parameters as well as damage extent and distribution. Convex shells with a response instability are found to have increased impact damage resistance compared with plates. A concept is proposed wherein the instability provides a mechanism, not available in plates, by which shell structures dissipate impact energy through structural deformation and thus exhibit improved impact damage resistance. Conversely, convex shells with no response instability have decreased impact damage resistance compared with plates. The differences in composite shell and plate behavior, particularly damage resistance, have important ramifications to the design of damage tolerant aerospace components and are discussed.

Introduction

DAMAGE resistance and tolerance of fibrous composite structures are significant concerns to the aerospace community due to the relatively low through-thickness strength and susceptibility of these structures to damaging events, e.g., impact. Therefore, the subjects of impact damage resistance and tolerance of composite structures have received considerable attention in recent years. Reviews of the current literature show, however, that there exists virtually no work concerning the impact damage resistance of composite shells, although composite plates have been explored extensively.[1–3] Unfortunately, structures such as wings and fuselages are more accurately characterized as shells, not plates, and thus the effects of initial curvature on the resulting impact response and damage resistance need to be explored.

The current work focuses on key phenomena in the response of composite shells to transverse loading with the overall goal being to explore the impact damage resistance of these structures. As convex shells are transversely loaded, an instability can result as the shell moves between two stable equilibrium paths.[4–6] Work with composite cylinders and shell sections (e.g., Refs. 7–10) has yielded useful results, but mechanistic explanations are sparse and inconclusive. Instabilities in the shell response were not reported and any difference in shell and plate response is generally attributed to the higher transverse stiffness (membrane) of the shells (e.g., Ref. 11). The impact response (including instability) of composite shells has been investigated analytically and experimentally, but the effect of the instability on the response characteristics, including damage extent, was not established.[11–14] Thus, a basic understanding of the loading/impact response (particularly damage resistance) of composite shells, including identification of important issues in the response, does not exist.

The baseline objective of the current work is thus to evaluate the response, including damage, of composite shell structures to transverse loading in impact and quasi-static testing. Basic structural and impact parameters were varied to determine the effect of each parameter on the resulting response, establish trends, and identify mechanisms that control the response. In the course of conducting this broad experimental investigation, an instability was observed to be particularly important in the response of convex shells. Therefore, a specific objective of the current paper is to establish differences in convex shell and plate response, including damage mode and extent, with particular focus on the instability aspect of the response. It is hoped that by documenting the instability in both impact and quasi-static tests that insights may be gained that lead to better predictive capabilities in the future.

Approach

An extensive experimental investigation, composed of impact and quasi-static testing, was undertaken to determine the response (including damage) of composite structures to transverse (centered) loading. Cylindrical composite shell structures were manufactured from Hercules AS4/3501-6 prepreg tape in a $[\pm 45_n/0_n]_s$ configuration where $n = 1$, 2, and 3. The cylindrical composite shell structures include convex and concave shell sections and plates (i.e., shells with a radius of ∞). The orientation of the ply angle with respect to specimen curvature is shown in Fig. 1.

As this work was considered an exploratory investigation, specimen structural parameters were varied to give a wide range of geometrical characteristics. Radius, span, and thickness were independently varied via scaling considerations. Scaling of the structural parameters is based on effective ply thickness, the total thickness of adjacent plies with the same fiber orientation. As the number of ply interfaces (between plies at different orientations) changes, delamination extent and distribution (through-thickness) change, thereby affecting the mix of different damage mechanisms.[15] This issue was avoided by utilizing effective plies to keep the number of ply interfaces constant despite different specimen thicknesses, thereby

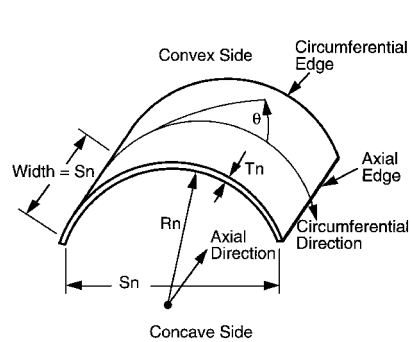

Fig. 1 Illustration of generic specimen.

Received Feb. 13, 1996; revision received Oct. 25, 1996; accepted for publication Nov. 10, 1996; also published in *AIAA Journal on Disc*, Volume 2, Number 2.

*Ph.D. Candidate, Technology Laboratory for Advanced Composites, Department of Aeronautics and Astronautics. Student Member AIAA.

†Professor and MacVicar Faculty Fellow, Technology Laboratory for Advanced Composites, Department of Aeronautics and Astronautics. Associate Fellow AIAA.

Table 1 Test matrix

	T1				T2				T3			
Span	R1	R2	R3	RP[a]	R1	R2	R3	RP	R1	R2	R3	RP
S1	4[b]	4	4	4	1	4	1	1	1	1	4	1
S2	4	1	1	—	—	1	—	—	—	1	1	—
S3	4	1	1	—	—	1	1	—	—	—	1	—
S1 concave	4	1	1	—	1	1	—	—	1	—	1	—

[a]RP indicates plates configuration (radius equal to ∞)
[b]Indicates one quasi-static test and number of impact tests at different velocities.

isolating changes in damage mode and extent to effects from structural parameters on the resulting response.

Using effective plies as the basis for scaling, three different values for each of the structural variables are obtained using the following relation:

$$X_n = n(X_1) \tag{1}$$

where X represents any of the three structural parameters, X_1 represents the base value for structural parameter X, and n takes on the values 1, 2, and 3. Base values for the structural parameters are R1 = 152 mm (6 in.), S1 = 102 mm (4 in.), and T1 = 0.804 mm. As an example, specimen R1S2T3 designates a specimen with nominal values of 152 mm for radius, 203 mm for span, and 2.412 mm (18 plies) for thickness. Intermediate values of span and thickness, i.e., S2 and T2, approximately correspond to values for stringer spacing (span) and thickness for a typical commercial aircraft.[16]

Impact velocities of 1, 2, 3, and 4 m/s were found to provide specimen responses ranging from purely elastic (no damage) to severe damage (specimen penetration) during preliminary testing. This range of response was deemed desirable from a damage resistance perspective and was therefore chosen for the test matrix. It was also found from preliminary tests that an impact velocity of 3 m/s would damage the majority of specimens in this investigation. Therefore, quasi-static tests were conducted until the maximum load measured during an impact test at 3 m/s of concomitant specimens was reached so that damage states resulting from impact and quasi-static tests could be compared based on peak force.[17,18]

The considerations of structural scaling along with the findings from preliminary testing were used to construct the test matrix presented in Table 1. The test matrix contains 89 specimens but is not fully populated. Attention was paid to the distribution of unpopulated entries in the test matrix so that information from testing could be used to establish trends that encompass unpopulated regions. Diagonals and border rows and columns are populated so that the behavior of interior unpopulated regions (specimens) can be interpolated, but not extrapolated, from the behavior of specimens that are tested.

During each impact test, the impactor force–time history was measured to determine the specimen response. Force–deflection histories were measured to characterize the response in the quasi-static tests. All specimens were visually evaluated for damage after testing and the dye-penetrant enhanced x-radiography method was utilized to determine the extent and distribution of nonvisible damage.

Experimental Specifics

An overview of the experimental procedures is given here, and detailed information can be found in Ref. 19. Specimen preparation and setup for the two types of loading (impact and quasi-static) are identical.

Specimen Preparation

Shells were manufactured using standard layup and cure procedures for this material system[20] except that the laminates were cured on specially designed cylindrical molds. Laminates were layed up by hand and processed using the standard manufacturer's cure cycle of a 1-h flow stage at 116°C and a 2-h set stage at 177°C. This was conducted in an autoclave under vacuum with a 0.59 MPa external pressure. Laminates were postcured in an oven at 177°C for 8 h and subsequently cut to the desired dimensions using a water-cooled diamond-grit cutting wheel. Specifics of the manufacturing procedure can be found in Ref. 19, including an evaluation of the manufacturing technique, which shows that the specimen quality is typical of standard plate specimens, i.e., average specimen thicknesses (and radii) are within 4% of the nominal values.

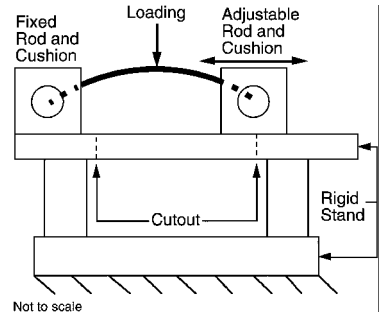

Fig. 2 Side-view illustration of test fixture with convex shell.

Test Fixture

The shells (and plates) are restrained in a specially designed test fixture with boundary conditions of pinned/no in-plane sliding (hinged) on the axial edges and free on the circumferential edges (edges defined in Fig. 1). Fixing the in-plane boundary condition exaggerates compressive membrane (in-plane) stresses developed in the initial loading of the convex shells, which is a basic (structural response) difference between convex shells and plates.

An overall view of the test fixture is presented in Fig. 2 for a convex shell. The test fixture consists of two primary components for restraining specimens along the axial edges: adjustable rods and cushions for the rods to rest in. Shells are restrained out of plane using steel knife edges, which actually have a 1.59 mm ($\frac{1}{16}$ in.) radius, that support the shell along the entire axial edge. The in-plane restraint is accomplished by the shell impinging on the flat face of the rod. Plates and concave shells require additional consideration (and attachments) because the in-plane condition at the boundary is tensile (pull-out), whereas for convex shells it is compressive (push-in) prior to the instability. The no sliding in-plane condition for these cases is attained by attaching extended knife edges to the axial plate edges.

A detailed description and performance evaluation of the test fixture can be found in Ref. 19, which shows the test fixture allows rotation at the pinned boundaries and adequately restrains the specimens (plates, concave, and convex shells) as desired.

Impact Testing

A device previously developed for impact testing of composite structures[21] was used to horizontally accelerate a steel impacting rod (total mass 1.60 kg) mounted in linear bearings to the desired velocities. A light-gate assembly is used to measure the impactor velocity (within $\pm$0.1 m/s) just prior to specimen contact. A force transducer, mounted behind a 12.7-mm ($\frac{1}{2}$-in.)-diam hemispherical steel tup on the impacting rod, measures load within $\pm$4.2 N (0.95 lb).

Because of the dynamic nature of the impact, the force measured by the transducer must be modified to account for the inertia of the tup.[22] In this investigation, the force on the tup (specimen) is 1.09 times the force measured by the transducer. Voltage output from the force transducer is digitized using a MacADIOS II analog/digital converter and recorded on a Macintosh IIx computer at 50 kHz. The measured force–time data can be twice integrated to give deflection–time data:

$$w(t) = \int_0^t \left[\int_0^t a(t)\,\mathrm{d}t + v_0 \right] \mathrm{d}t + x_0 \tag{2}$$

where $w(t)$ is deflection, $a(t)$ is the modified (to account for the tup inertia) force–time history divided by the mass of the impacting assembly, t is time, v_0 is the measured initial velocity, and x_0 is the initial specimen deflection, which is zero. The integrations are performed using the trapezoidal rule where the time step is equal to the data-sampling interval of 20 μs.

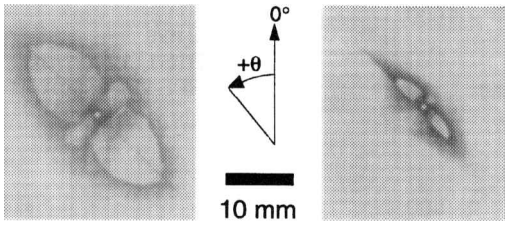

Fig. 3 Typical x-radiographs of damage: shown are specimen types R1S1T3 (concave) impacted at 3 m/s (left) and RPS1T1 (plate) impacted at 2 m/s (right).

Quasi-Static Testing

Quasi-static testing was performed with an MTS-810 uniaxial testing machine under stroke (deflection) control. An MTS 8896-N (2000-lb) load cell is used to measure the force on the specimen, and the stroke of the testing machine is used to measure deflection. Force resolution for quasi-static testing is 0.9 N (0.2 lb), whereas the deflection resolution varies with stroke range but is always better than $\pm$0.06 mm. Peak force is known a priori for each test from the impact tests at 3 m/s, and peak deflection is estimated using Eq. (2) to obtain an approximate stroke range for each test. The stroke rate is set so that loading and unloading each lasts 3 min, giving a total test time of 6 min for each specimen. Data are sampled at 2 Hz with the same data acquisition system previously described. Although not reported here, indentation of the specimens was also measured using a linearly variable differential transformer displacement transducer placed directly under the indentor.

Damage Evaluation

Dye-penetrant enhanced x-radiography[23,24] and visual inspection were used to characterize damage.[19] Dye-penetrant was injected via a syringe into a 0.79-mm-diam hole drilled through the damage area. A piece of flash tape was placed on the back surface of the specimens to contain the dye. This technique allows an integrated view of delamination and matrix cracking. Typical delaminations and matrix cracks extend in the +45- and $-$45-deg directions, with the +45-deg direction always having a greater extent, as shown in the sample x-radiographs provided in Fig. 3. Two damage metrics were defined for use with the planar x-radiograph view of the damaged specimen. The delamination lengths in the +45- and $-$45-deg directions were measured to the nearest millimeter and then averaged to quantify the extent of the damage. This yields an average damage extent metric. The ratio of delamination length in the $-$45-deg direction to that in the +45-deg direction yields a damage extent ratio, which is used to quantify the distribution of damage. The average damage extent and damage extent ratio for the two specimens shown in Fig. 3 are, respectively, 20 mm and 0.44 (R1S1T3 concave) and 8 mm and 0.33 (RPS1T1).

Results and Discussion

In the following discussion, quasi-static data are used interchangeably with impact data. This is done because the impact and quasi-static response (including damage) are equivalent for these specimens,[19] given that the peak force of the tests for each specimen type were the same. This equivalence has also been documented for composite plates subjected to low-velocity impact.[25–27] Furthermore, this facilitates characterization in a number of cases when response characteristics are more easily discerned in the quasi-static data than in the impact data due to noise inherent in the impact data from impactor vibration.

Loading Response

The instability in convex shell response is illustrated in Fig. 4. Displacement w is nondimensionalized using the specimen thickness to illustrate the large-deflection behavior. The loading initially increases with deflection along a nonlinear path, termed the first equilibrium path. The load reaches a local maximum, termed the critical snapping load, before decreasing as deflection increases into the instability region. The response then progresses along a second equilibrium path to the maximum force (and deflection) of this test.

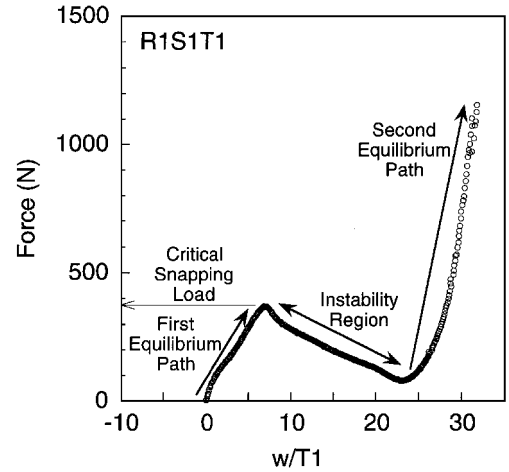

Fig. 4 Illustration of definitions used to describe instability characteristics (data from quasi-static test of specimen R1S1T1).

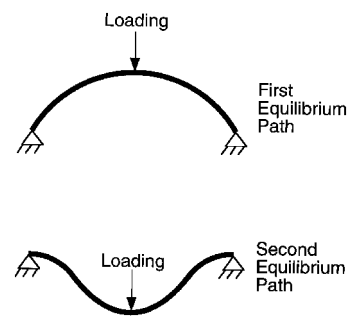

Fig. 5 Illustration of convex shell cross section under loading: top, in the first equilibrium position; and bottom, in the second (concave) equilibrium position.

The deformation modes of the convex shells are quite different for the first and second equilibrium paths as illustrated in Fig. 5. Along the first equilibrium path, the convex shell is in the initial (convex) configuration, whereas along the second equilibrium path the shell is in an inverted (concave) configuration. By contrast, plate specimens load monotonically (with nonlinear stiffening due to large-deflection membrane effects) and slowly take on a concave shape; i.e., plates do not possess an instability. It should be noted that, although none were observed, unsymmetric (with respect to the loading axis) deformation modes are possible.

Although the response found in this work resembles a snap-through instability, it is clearly different in one respect. Snap-through instabilities progress along an equilibrium path until a critical load (local maximum) is reached, oftentimes referred to as the buckling load, where the shell configuration dynamically transitions from convex to concave. This dynamic transition is characteristic of a load-controlled test. However, the impact response observed in this investigation contains a stable path between the first and second equilibrium paths with no instantaneous "snapping." This instability response, with the lack of dynamic snap-through, shows impact to be a deflection-controlled event.

Effects of the instability, clearly evident in the resultant force–time histories of impacted convex shells, are not observed in plate force–time histories. A typical plate force–time history, oftentimes referred to as a half-sinusoid response in the literature, is presented in Fig. 6 for specimen RPS1T1 impacted at 1 m/s. This typical plate behavior can be contrasted with the behavior of a convex shell (specimen type R1S1T1) impacted at different initial velocities to illustrate the effect of the instability. The convex shell (R1S1T1) response to an impact at 1 m/s is also presented in Fig. 6 and is noted to be quite similar to the plate (RPS1T1) response. However, the response of the convex shell to an impact at 2 m/s, presented in Fig. 7, shows a dramatic change in the response in that three local maxima and two local minima are evident.

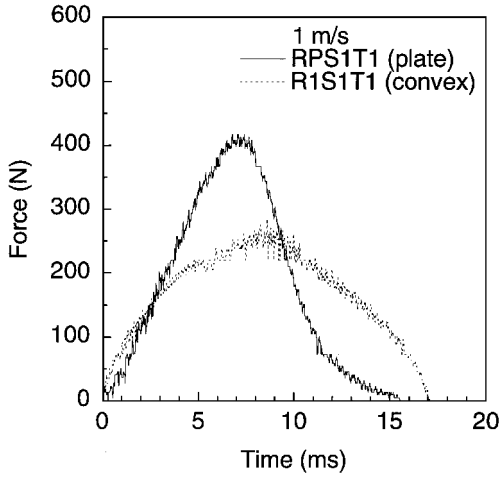

Fig. 6 Force–time response of plate (RPS1T1) and convex shell (R1S1T1) specimens impacted at 1 m/s.

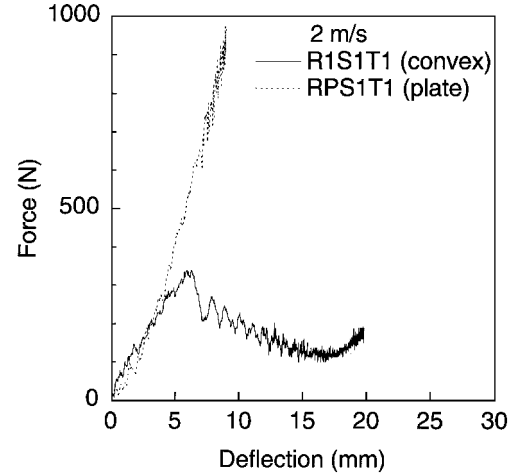

Fig. 8 Force–deflection response of specimen types R1S1T1 (convex) and RPS1T1 (plate) impacted at 2 m/s.

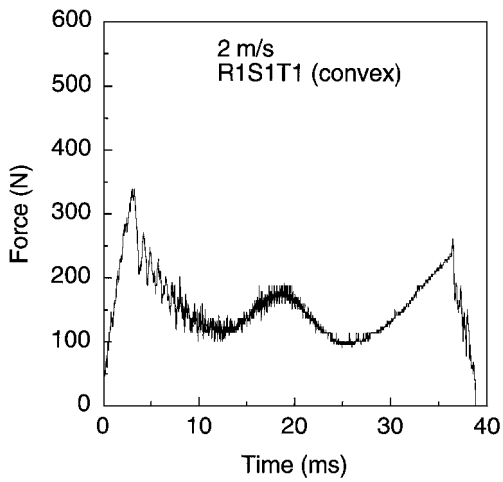

Fig. 7 Force–time response of specimen R1S1T1 impacted at 2 m/s, displaying effect of the instability.

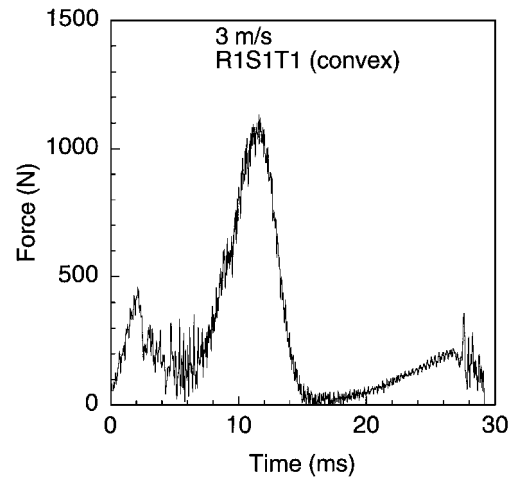

Fig. 9 Force–time response of specimen R1S1T1 impacted at 3 m/s.

The effect of the instability can be more clearly discerned by considering the force–deflection response shown in Fig. 8, which corresponds to the force–time data in Fig. 7. The first peak in the force–time data (Fig. 7) corresponds to the point on the first equilibrium path in Fig. 8 where the shell response reaches the critical snapping load. The force then decreases with time (displacement still increasing) as the shell moves into the instability region. The second peak, at approximately 19 ms, occurs when the shell response begins to load onto the second equilibrium path. No damage was observed in the x-radiograph for this specimen, which would indicate that unloading would follow the loading curve, i.e., there is little hysteresis. This is indicated by the nearly symmetric nature of the force–time history.

Thus, for the case of the convex shell specimen impacted at 2 m/s, the impactor had enough energy to cause the shell to deflect past the critical snapping load (of approximately 350 N) and into the instability region. This is in contrast to the same specimen type impacted at 1 m/s where the peak force reached approximately 290 N such that the specimen did not progress beyond the first equilibrium path or display any characteristics of an instability.

The effect of the instability is further demonstrated by considering the force–deflection response of specimen RPS1T1 (plate), also impacted at 2 m/s and presented in Fig. 8. The only difference between the two specimens in Fig. 8 is the curvature of the convex shell, but the response is clearly quite different—thus indicating the strong effect of shell curvature and the resulting instability on the response.

The response of specimen type R1S1T1 impacted at 3 m/s, presented in Fig. 9, displays the same minima and maxima as the response to the impact at 2 m/s. At higher velocities for specimen type R1S1T1, the response progresses farther onto the second equilibrium path and occurs over a shorter time. The noted difference is that the second local maximum, i.e., the loading on the second equilibrium path, is now greater than the other two local maxima (critical snapping load), making it the peak force for the impact event. This is seen in Fig. 9 where the peak force is much higher in the impact at 3 m/s compared with the impact at 2 m/s (see Fig. 7). A significant amount of damage is observed in the x-radiograph of specimen type R1S1T1 impacted at 3 m/s. The impact response for this specimen shows a lack of symmetry in the unloading (see Fig. 9). At an impact velocity of 4 m/s, specimen type R1S1T1 (convex) was penetrated. The force–time history for the impact at 4 m/s exhibits the same characteristic features of the impact at 3 m/s until penetration. As is typical in composite plate impact, the measured force drops dramatically at penetration (sometimes referred to as perforation).

It is important to note that the onset of the instability is nearly indiscernible in the deflection–time histories, even when the instability is clearly evident in the force–time and force–deflection histories. The deflection–time histories for a plate (no instability) and a convex shell, with and without an instability, are presented in Fig. 10 to illustrate this. The shape of the deflection–time histories are indistinguishable from one another, although the magnitude of the convex shell deflection is generally much greater than the plate for the same impact event. The force–time history for specimen R1S1T1 (convex) impacted at 2 m/s (see Fig. 7) clearly indicates an instability, whereas the other force–time histories do not. Therefore, deflection–time histories alone generally are not adequate to describe shell response.

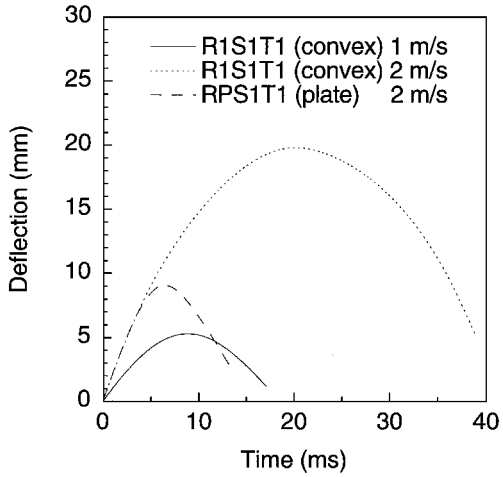

Fig. 10 Deflection–time histories for specimen types RPS1T1 and R1S1T1.

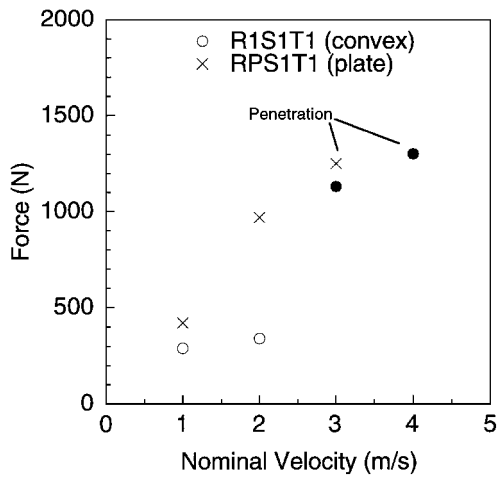

Fig. 11 Peak impact force vs nominal impact velocity for specimen types R1S1T1 (convex) and RPS1T1 (plate). Note: filled data points indicate peak force on the second equilibrium path.

Quantitative differences are also used to elucidate effects of the instability. Parameters from the impact response, such as peak force and contact time, have been used to characterize the response of plates to impact loading. For plates, peak impact force increases linearly and contact time decreases nonlinearly with velocity up to penetration.[15,28] Results from this investigation indicate that convex shells with an instability do not follow the same trends as plates. The variation in peak impact force with velocity for specimen types R1S1T1 (convex) and RPS1T1 (plate) is presented in Fig. 11. The instability is strongly associated with the departure from a linear increase in peak force with velocity for the convex shell. This is indicated in Fig. 11 by separating the data into events where the load does and does not progress past the value of the critical snapping load on the second equilibrium path. This distinction indicates on which equilibrium path the peak force occurs. Between the impact at 1 and 2 m/s, the convex shell transitions into the instability region without an increase in peak force, whereas the plate specimen continues to a much higher load (along a monotonic, stiffening load–deflection curve). The nonlinearly decreasing trend of contact time with velocity found for plates[28] is also not observed for convex shells. For example, the contact time actually increases between impact velocities of 1 and 2 m/s for convex shell R1S1T1 (see Figs. 6 and 7), again due to the transition through the instability region between equilibrium paths.

Note that although the results presented up to this point are typical of many convex shells in this investigation, all shells do not respond in exactly the same manner. All the structural parameters considered were found to affect the instability region, i.e., the critical snapping load and the extent (with respect to deflection) of the instability region. The instability was most evident in specimens with larger radii and smaller thicknesses (T1 or T2) but was not observed for any of the thickest T3 (2.412 mm) specimens. This is most likely due to the higher bending stiffness of the thicker shells. Parameters that quantify the effect of structural parameters on the instability are beyond the scope of this paper. However, results and trends show that specimens with structural parameters that most closely approximate an aircraft fuselage are strongly affected by the instability. These specimens have large radius, intermediate span, and intermediate thickness. For example, a Boeing 757 fuselage has a radius of 1.88 m (74 in.) and a stringer spacing of 229 mm (9 in.) (Ref. 16). A composite aircraft fuselage can have a thickness as small as 1.5 mm (Ref. 29).

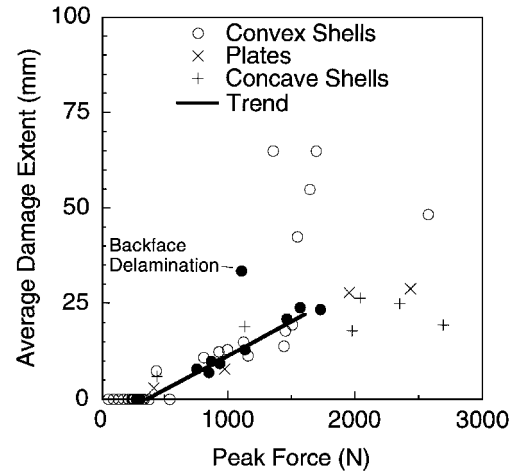

Fig. 12 Average damage extent vs peak force for impacted specimens. Note: filled data points indicate peak force on the second equilibrium path.

Impact Damage Response

A strong correlation between peak force and damage resistance has previously been demonstrated by several authors[17,18] for impacted composite plates. The average damage extent (damage resistance metric) vs peak force is presented in Fig. 12 for all plate, convex, and concave shell specimens impacted in this investigation (quasi-static data agree with these data). Convex shell data are separated by the equilibrium path on which the peak load occurs. Penetrated specimens are not included because the average damage extent metric has little or no meaning for specimens that are penetrated. Despite the instability, the average damage extent for convex shells was found to scale nearly linearly over a large range of peak forces (below approximately 1500 N), as shown in Fig. 12. A line is sketched in Fig. 12 to indicate this nearly linear behavior. All specimens exhibit a damage threshold force of approximately 400 N, below which no damage is found. The average damage extent for plates and concave shells is noted to increase nearly linearly with peak force over the entire range, whereas convex shells which do not progress past the critical snapping load and remain on the first equilibrium path display significantly increased average damage extent above approximately 1500 N.

This increased damage extent for convex shells that reach high peak loads on the first equilibrium path is attributed to compressive membrane stresses that have been shown to promote delamination growth through sublaminate buckling.[30,31] Convex shells on the first equilibrium path experience compressive membrane stresses, whereas the other specimen geometries, including convex shells on the second equilibrium path and plates, experience tensile membrane stresses. The increased delamination extent can be seen in Fig. 13 for specimen R1S1T3 (convex) with the peak force on the first equilibrium path (and with no instability) as contrasted with specimen R2S1T2 (convex) with the peak force on the second equilibrium path. These specimens have approximately the same peak force of 1700 N. Convex shells that remain on the first equilibrium path at high loads all have larger thicknesses and therefore higher

Table 2 Average damage extent ratio for impact and quasi-static tests

	Impact	Quasi-static
Convex (first equilibrium path)	0.63	0.64
Convex (second equilibrium path)	0.34	0.34
Concave	0.49	0.44
Plate	0.30	0.32

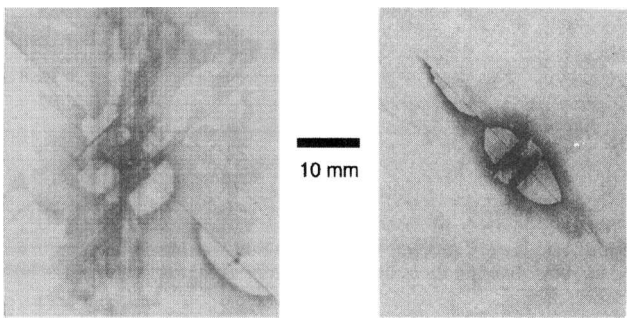

Fig. 13 X-radiographs of convex shell specimens R1S1T3 impacted at 3 m/s (left) and R2S1T2 impacted at 4 m/s (right), each having peak force of approximately 1700 N.

bending stiffnesses, which allow higher peak forces to be reached on the first equilibrium path.

Differences in damage distribution are also attributed to the presence of compressive vs tensile membrane stresses. The overall difference in the damage can be seen in Fig. 13, where the convex shell with compressive membrane stresses at peak load is noted to have a nearly symmetric damage distribution with respect to the +45- and −45-deg directions, whereas the other shell has preferential damage extent in the +45-deg direction. The differences in damage distribution are quantified using the damage extent ratio metric as averaged in Table 2. The average damage extent ratios for convex shells with peak force on the first equilibrium path are nearly double that for those with peak force on the second equilibrium path. Furthermore, convex shells with peak force on the first equilibrium path have the highest average damage extent ratio of all specimens.

Significant compressive membrane stresses can increase the damage extent and affect the damage distribution by causing delamination growth due to sublaminate buckling. The critical snapping load and instability thus affect the resulting damage because the sense (compressive or tensile) and magnitude of the membrane stress depend upon the peak force and on which equilibrium path it occurs.

Implications for Damage Resistance

The instability has two primary implications for the impact damage resistance of composite structures. First, convex composite shell structures that reach high peak loads on the first equilibrium path (no instability effects) have increased damage extent and different damage modes than equivalent plates. These structures are therefore less damage resistant than plates and using plate data for design is not conservative. Second, given an impact event, convex composite structures that do transition through the instability are noted to have decreased damage extent compared with plates, thus giving such convex shell structures increased damage resistance compared with plates.

This latter point can be explained by recalling that damage extent scales with peak impact force and, therefore, increased impact damage resistance will be realized if, given an impact event, lower peak forces result. During impact, impactor kinetic energy is consumed by the rebound energy of the impactor, structural or strain energy (work done in deforming the specimen), damage energy, and higher-order effects such as noise and heat generation. External applied loads acting through specimen displacements (work) are the only contributions to the structural strain energy created during impact. As these impact events are known to be quasi-static in nature,[19] the strain energy absorbed by a structure during impact is related to the external applied tractions and displacements via

$$\int_V \left(\int \sigma_{ij}\, \mathrm{d}\varepsilon_{ij} \right) \mathrm{d}V = \int_S \left(\int T_i\, \mathrm{d}u_i \right) \mathrm{d}S \qquad (3)$$

where T_i and u_i are the resolved external applied tractions and displacements, respectively, σ_{ij} is the stress tensor, ε_{ij} is the strain tensor, and S and V are the surface and volume of the structure, respectively. Assuming ideal boundary conditions (i.e., zero moment and zero displacement), no work is done at the boundary of the shells, leaving only the contribution due to the impactor.

It is hypothesized that convex shells with an instability have increased impact damage resistance compared with plates due to the large amount of impact energy consumed in transitioning through the instability region (with large structural deformations), as opposed to energy consumption through high peak forces. High peak forces tend to result in increased damage as has been previously established.

The work/energy contribution can be calculated, using Eq. (3), by idealizing the impactor effect as a point force equal to the measured force acting through the displacement of the impactor. Specimen displacement can be calculated using Eq. (2). Thus, the impactor energy absorbed by the structure (strain energy) is idealized as the area under the force–deflection history up to the maximum specimen deflection. As with deflections in the impact tests, this area (energy) can be calculated using the trapezoidal rule. The critical snapping load and the deflection(s) associated with the instability region are therefore important parameters because the amount of energy consumed by the instability scales with these quantities.

The impact force–deflection response to impacts at 2 m/s for specimens R1S1T1 (convex) and RPS1T1 (plate), already presented in Fig. 8, provides a convincing example of the improved impact resistance. The only difference between the two specimens is the radius of curvature (152 mm for the convex shell and ∞ for the plate). The convex shell reaches a substantially smaller peak force (approximately 350 N) and was not damaged, whereas the plate reached a much higher peak force (approximately 1000 N) and was significantly damaged (see x-radiograph in Fig. 3). Utilizing the procedure established for calculating the work contribution, the results show that the convex shell and plate consume approximately the same amount of energy, 3.5 and 3.4 J, respectively. Thus, the shell is able, through the instability mechanism, to absorb the impact energy through large displacements, whereas the plate absorbs the energy through high peak loads. The higher peak force for the plate results in greater potential for damage formation and actual manifestation of increased damage extent.

The effect of the instability on the resultant peak force can be further illustrated by considering the progress of specimens impacted at different velocities (energies) along the representative quasi-static load–deflection curves. The dashed lines and velocities in Figs. 14 and 15 indicate the peak force (and location) that specimen types R1S1T1 (convex) and RPS1T1 (plate) attained during impact testing. It can be seen that the peak force increases at a greater rate with velocity for the plate than for the shell, leading to increased damage in the plate for a given impact event. Furthermore, the impacts of specimen R1S1T1 (convex) at 1 and 2 m/s result in a nearly identical peak force, even though the impactor energy increased by a factor of 4 (0.8 and 3.5 J, respectively), thus demonstrating the ability to consume energy through deflections associated with the instability. Neither of these convex specimens were damaged (lower peak force), whereas the plate specimen was damaged in the impact at 2 m/s (higher peak force).

The instability in convex shell response thus gives convex shell structures improved impact damage resistance over plates. This implies that damage resistance is a structural parameter and further indicates that there are structural concepts that can be utilized to design for improved damage resistance. By using these structural concepts, damage tolerance of composite structures can also be positively affected. These composite structures can take advantage of the gross structural response, specifically the instability, to dissipate impact energy and maintain low impactor loads because the impact response occurs on a structural scale. This is in contrast to

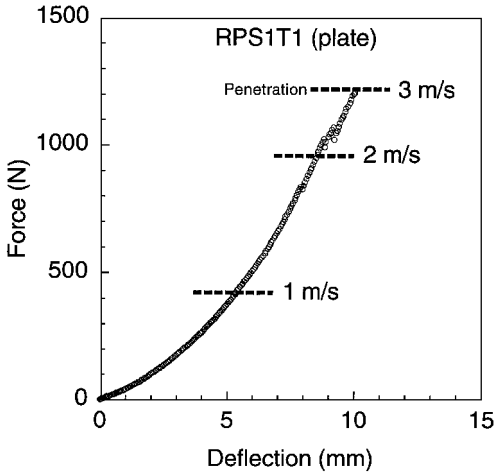

Fig. 14 Quasi-static force–deflection loading response of specimen RPS1T1 (plate) and corresponding impact velocities.

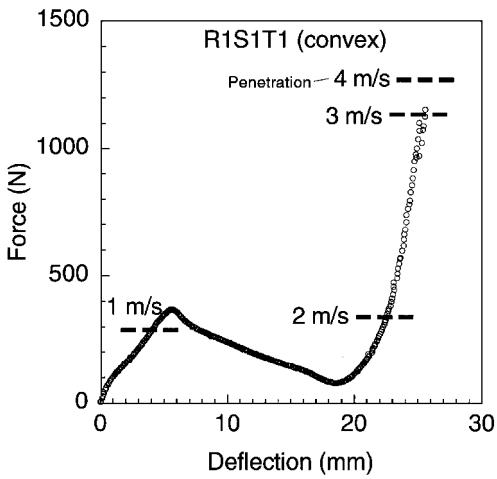

Fig. 15 Quasi-static force–deflection loading response of specimen R1S1T1 (convex) and corresponding impact velocities.

thin-gauge metallic (e.g., aluminum) structures where the response to impact is oftentimes dominated by local effects such as plasticity; i.e., sheet metals dent more easily than composites.[32]

The manifold effects of the instability outlined in the previous section clearly show that the instability is an important aspect of shell impact response. Plate impact response, including the resulting damage, is thus found to be significantly different than that of convex shells due to this instability. Therefore, the sizable understanding and database accumulated on composite plate impact response must be utilized carefully when those data are applied to structures that are more appropriately modeled as shells because effects of the instability must be considered.

Summary

Through an experimental study of composite structures, substantial differences in plate and convex shell response to transverse loading have been established. An instability in the loading response of convex shells is noted to be the source of these differences and thus to have a strong influence on the impact response of these composite structures, including damage (impact damage resistance). Because of this unstable nature of the convex shell response, an additional crucial parameter in characterizing impact response is the critical snapping load. This critical snapping load acts as a demarcation between a monotonic loading response and one with an instability. The instability is shown to influence the shape of both force–deflection and force–time histories, as well as trends. Therefore, trends previously established for impacted composite plates do not hold for convex shells, and in some cases, the trends can even reverse.

With regard to impact damage, the instability has two primary effects. First, unlike composite plates that display a nearly linear damage progression with peak force, impacted convex shells have been found to deviate from this progression if high peak forces are reached prior to the onset of instability. In these cases, compressive membrane stresses are present and the damage extent is shown to increase significantly over the nearly linear trend. This is attributed to increased delamination extent induced by the compressive membrane stresses. Thus, decreased impact damage resistance is observed for these types of composite shells compared with plates. This is in contrast to the second effect of the instability on damage where convex shells which transition through the instability region are shown to have increased (improved) impact damage resistance compared with plates. Convex shells with an instability consume impact energy through large deflections in the instability region. Plates do not experience an instability, and therefore this mechanism of impact energy consumption is not available. Thus, plates reach higher peak forces, which results in (increased) damage. This insight into the impact damage resistance of composite shell structures is important in understanding and designing damage resistant and damage tolerant composite structures.

It is clear that the instability in convex shell response affects the resultant damage, which implies that damage resistance is, itself, a structural parameter. However, effects of structural parameters (specimen geometry) on the instability of composite shells and the resulting response (including damage) need to be explored further. Likewise, specifics of the damage state and parameters that contribute to the mode(s) of damage formation have not yet been clearly identified. Further work in this area, as well as in establishing the mechanisms by which different stress states in convex shells (as a result of the instability) affect the resultant damage, is crucial to gaining a greater understanding of damage resistance. In particular, tensile and compressive membrane stresses in composite shells need to be analyzed for their role in damage formation. Such work will lead to a better understanding of the role of instability in the impact response of composite shells.

Acknowledgments

This work was sponsored by the Federal Aviation Administration under Research Grant 94-G-037 and the NASA Langley Research Center under NASA Grant NAG-1-991.

References

[1]Abrate, S., "Impact on Laminated Composite Materials," *Applied Mechanics Review*, Vol. 44, No. 4, 1991, pp. 155–190.

[2]Abrate, S., "Impact on Laminated Composites: Recent Advances," *Applied Mechanics Review*, Vol. 47, No. 11, 1994, pp. 517–544.

[3]Cantwell, W. J., and Morton, J., "The Impact Resistance of Composite Materials," *Composites*, Vol. 22, No. 5, 1991, pp. 55–97.

[4]Marshall, I. H., Rhodes, J., and Banks, W. M., "Experimental Snap-Buckling Behaviour of Thin GRP Curved Panels Under Lateral Loading," *Composites*, Vol. 8, April 1977, pp. 81–86.

[5]Marshall, I. H., Rhodes, J., and Banks, W. M., "The Nonlinear Behaviour of Thin, Orthotropic, Curved Panels Under Lateral Loading," *Journal of Mechanical Engineering Science*, Vol. 19, No. 1, 1977, pp. 30–37.

[6]Marshall, I. H., and Rhodes, J., "Snap-Buckling of Thin Shells of Rectangular Planform," *Stability Problems in Engineering Structures and Components*, edited by T. H. Richards and P. Stanley, Applied Science Publisher, London, 1979, pp. 249–264.

[7]Manders, P. W., Bader, M. G., Hinton, M. J., and Flower, P. Q., "Mechanisms of Impact Damage in Filament Wound Glass-Fibre/Epoxy-Resin Tubes," *Third International Conference on Mechanical Behaviour of Materials*, Pergamon, New York, 1979, pp. 275–284.

[8]Christoforou, A. P., Swanson, S. R., Ventrello, S. C., and Beckwith, S. W., "Impact Damage of Carbon/Epoxy Composite Cylinders," *32nd International SAMPE Symposium and Exhibition*, Society for the Advancement of Materials and Process Engineering, Covina, CA, 1987, pp. 964–973.

[9]Palazotto, A., Perry, R., and Sandhu, R., "Impact Response of Graphite/Epoxy Cylindrical Panels," *AIAA Journal*, Vol. 30, No. 7, 1992, pp. 1827–1832.

[10]Perry, R. B., "Impact Damage in Curved Graphite/Epoxy Panels with Clamped Edges," M.S. Thesis, School of Engineering, Air Force Inst. of Technology, Wright–Patterson AFB, OH, 1990.

[11]Lin, H. J., and Lee, Y. J., "Inelastic Impact of Composite Laminated Plate and Shell Structures," *Composite Structures*, Vol. 14, No. 2, 1990, pp. 89–111.

[12]Lin, H. J., and Lee, Y. J., "Impact-Induced Fracture in Laminated Plates and Shells," *Journal of Composite Materials*, Vol. 24, Nov. 1990, pp. 1179–1199.

[13]Kistler, L. S., "Experimental Investigation of the Impact Response of Cylindrically Curved Laminated Composite Panels," *Proceedings of the AIAA/ASME/ASCE/AHS/ASC 35th Structures, Structural Dynamics, and Materials Conference*, AIAA, Washington, DC, 1994, pp. 2292–2297.

[14]Palazotto, A. N., Chien, L. S., and Taylor, W. W., "Stability Characteristics of Laminated Cylindrical Panels Under Transverse Loading," *AIAA Journal*, Vol. 30, No. 6, 1992, pp. 1649–1653.

[15]Lagace, P. A., and Wolf, E., "Impact Damage Resistance of Several Laminated Material Systems," *Proceedings of the AIAA/ASME/ASCE/AHS/ASC 34th Structures, Structural Dynamics, and Materials Conference*, AIAA, Washington, DC, 1993, pp. 1863–1872.

[16]Niu, M. C. Y., *Airframe Structural Design—Practical Design Information and Data on Aircraft Structures*, 8th ed., Conmilit Press Ltd., Los Angeles, CA, 1995, pp. 384–389.

[17]Jackson, W. C., and Poe, C. C., Jr., "The Use of Impact Force as a Scale Parameter for the Impact Response of Composite Laminates," *Journal of Composites Technology and Research*, Vol. 15, Winter 1992, pp. 282–289.

[18]Lagace, P. A., Williamson, J. E., Tsang, P. H. W., Wolf, E., and Thomas, S. A., "The Use of Force as a (Impact) Damage Resistance Parameter," *American Society for Composites Seventh Technical Conference* (University Park, PA), Technomic, Lancaster, PA, 1992, pp. 991–1000.

[19]Wardle, B. L., "Impact and Quasi-Static Response of Cylindrical Composite Shells," Technology Lab. for Advanced Composites, TELAC Rept. 95-4, Massachusetts Inst. of Technology, Cambridge, MA, 1995.

[20]Lagace, P. A., Brewer, J. C., and Varnerin, C., "TELAC Manufacturing Course Notes," Massachusetts Inst. of Technology, Technology Lab. for Advanced Composites, TELAC Rept. 88-4B, Cambridge, MA, 1990.

[21]Lie, S. C., "Damage Resistance and Damage Tolerance of Thin Composite Facesheet Honeycomb Panels," Technology Lab. for Advanced Composites, TELAC Rept. 89-3, Massachusetts Inst. of Technology, Cambridge, MA, 1989.

[22]Ryan, K. F., "Dynamic Response of Graphite/Epoxy Plates Subjected to Impact Loading," Technology Lab. for Advanced Composites, TELAC Rept. 89-13, Massachusetts Inst. of Technology, Cambridge, MA, 1990.

[23]Freeman, S. M., "Characterization of Lamina and Interlaminar Damage in Graphite/Epoxy Composites by the Deply Technique," *Composite Materials: Testing and Design*, ASTM STP 787, American Society for Testing and Materials, Philadelphia, PA, 1982, pp. 50–62.

[24]Chang, F. H., Couchman, J. C., Eisenmann, J. R., and Lee, B. G. W., "Application of a Special X-Ray Nondestructive Testing Technique for Monitoring Damage Zone Growth in Composite Laminates," *Composite Reliability*, ASTM STP 580, American Society for Testing and Materials, Philadelphia, PA, 1975, pp. 176–190.

[25]Tan, T. M., and Sun, C. T., "Use of Statical Indentation Laws in the Impact Analysis of Laminated Composite Plates," *Journal of Applied Mechanics*, Vol. 52, March 1985, pp. 6–12.

[26]Lagace, P. A., Williamson, J. E., Tsang, P. H. W., Wolf, E., and Thomas, S., "A Preliminary Proposition for a Test Method to Measure (Impact) Damage Resistance," *Journal of Reinforced Plastics and Composites*, Vol. 12, May 1993, pp. 584–601.

[27]Lee, S., and Zahuta, P., "Instrumented Impact and Static Indentation of Composites," *Journal of Composite Materials*, Vol. 25, Feb. 1991, pp. 204–222.

[28]Wolf, E., "Impact Damage Mechanisms in Several Laminated Material Systems," Technology Lab. for Advanced Composites, TELAC Rept. 92-3, Massachusetts Inst. of Technology, Cambridge, MA, 1992.

[29]Quinlivan, J. T., Wilson, R. D., Smith, P. J., and Johnson, R. W., "ACEE Composite Structures Technology," NASA-CR-172358, Boeing Commercial Airplane Co., Aug. 1984.

[30]Cairns, D. S., Minguet, P. J.-A., and Abdallah, A. G., "Theoretical and Experimental Response of Composite Laminates with Delaminations Loaded in Compression," *Proceedings of the AIAA/ASME/ASCE/AHS/ASC 33rd Structures, Structural Dynamics, and Materials Conference*, AIAA, Washington, DC, 1992, pp. 1–9.

[31]Whitcomb, J. D., "Mechanics of Instability-Related Delamination Growth," NASA TM-100622, May 1988.

[32]Reinhart, T. J., "Introduction to Composites," *Composites*, edited by C. A. Dostal, M. S. Woods, and A. W. Ronke, Vol. 1, Engineered Materials Handbook, ASM International, Metals Park, OH, 1989, pp. 35, 36.